Special Issue Article

Advances in Mechanical Engineering

Advances in Mechanical Engineering
2015, Vol. 7(12) 1–8

DOI: 10.1177/1687814015619831
aime.sagepub.com
SAGE

Visualizing control systems performance: A fractional perspective

António M Lopes[1] and José A Tenreiro Machado[2]

Abstract

This article presents a novel method for visualizing the control systems behavior. The proposed scheme uses the tools of fractional calculus and computes the signals propagating within the system structure as a time/frequency-space wave. Linear and nonlinear closed-loop control systems are analyzed, for both the time and frequency responses, under the action of a reference step input signal. Several nonlinearities, namely, Coulomb friction and backlash, are also tested. The numerical experiments demonstrate the feasibility of the proposed methodology as a visualization tool and motivate its extension for other systems and classes of nonlinearities.

Keywords

Control system, fractional calculus, signal propagation, visualization

Date received: 14 September 2015; accepted: 4 November 2015

Academic Editor: Xiao-Jun Yang

Introduction

Linear control theory is a well-established matter, and a plethora of methods for the analysis and synthesis of linear systems has been developed.[1–4] However, linear systems are far from being the most adequate models of real-world phenomena since most exhibit nonlinear behavior. Due to this fact, during the last decade, researchers have paid more attention to nonlinear methods, but the available mathematical tools are complex and far from leading to straightforward results.[5–11]

In this article, we propose a methodology for observing the performance of control systems. The scheme is a pure mathematical and numerical formulation, and the results are to be interpreted as a new visualization concept inspired in the fractional calculus (FC). In this line of thought, the goal of the study is not to obtain a physical meaning but to open a new alternative concept to the classical integer modus operandi. The method computes the signal that propagates within the structure of a control system, leading to the representation of the traveling signal in both the time and frequency domains.

Having these ideas in mind, this article is organized as follows. In section "Mathematical tools," we present the main mathematical tools for processing data. In section "Numerical simulation and computer visualization," we simulate the system dynamics, and we propose a methodology for visualizing signal-wave propagation. Finally, in section "Conclusion," we outline the main conclusions.

Mathematical tools

In this section, we present the main mathematical tools to be adopted during the data processing. Hence, in

[1]UISPA–LAETA/INEGI, Faculty of Engineering, University of Porto, Porto, Portugal
[2]Department of Electrical Engineering, Institute of Engineering, Polytechnic of Porto, Porto, Portugal

Corresponding author:
António M Lopes, UISPA–LAETA/INEGI, Faculty of Engineering, University of Porto, Rua Dr. Roberto Frias, 4200-465 Porto, Portugal.
Email: aml@fe.up.pt

sub-section "Fractional-order derivatives and integrals," we introduce briefly the concept of fractional-order "differintegral." In sub-sections "Fourier transform" and "Fractionalization of elemental blocks," we recall the Fourier transform (FT) operator and we address the fractionalization of an elemental linear block, respectively.

Fractional-order derivatives and integrals

FC generalizes the concepts of derivative and integral to non-integer orders. During the last decades, FC was found to play a fundamental role in modeling many relevant physical phenomena and emerged as an important tool in the area of dynamical systems with complex behavior.[12–20]

In a loose sense, fractional derivatives and integrals "interpolate" between integer-order operators. This property is particularly useful in control engineering since we can adapt standard algorithms to a smoother version based on FC. Besides this aspect, FC operators capture memory effects, which make them an useful tool in the modeling of phenomena with long-range correlations and memory.

Several definitions of fractional derivative and integral have been proposed.[21–23] We recall here the Grünwald–Letnikov (GL) fractional "differintegral" operator of order $\alpha \in \mathbb{R}$, ${}_a^{GL}D_t^{\alpha}$, given by[24]

$$ {}_a^{GL}D_t^{\alpha} f(t) = \lim_{h \to 0} h^{-\alpha} \sum_{m=0}^{\left[\frac{t-a}{h}\right]} (-1)^m \binom{\alpha}{m} f(t - mh) \tag{1} $$

where $[\cdot]$ denotes the integer part, h is the time increment, and $\{t, a\} \in \mathbb{R}$ are the upper and lower limits of the "differintegral" operation.

Using the Laplace transform and neglecting initial conditions, we have the expression

$$ \mathcal{L}\left\{ {}_0^{GL}D_t^{\alpha} f(t) \right\} = s^{\alpha} \mathcal{L}\{f(t)\} \tag{2} $$

where s and $\mathcal{L}\{\cdot\}$ represent the Laplace variable and operator, respectively.

The Mittag-Leffler (ML) function, $E_{\alpha}(t)$, plays an important role in the context of FC, being defined by

$$ E_{\alpha}(t) = \sum_{m=0}^{\infty} \frac{t^m}{\Gamma(\alpha m + 1)} \tag{3} $$

This function establishes a connection between purely exponential and power law behaviors that characterize integer and fractional-order phenomena, respectively.[18] In particular, if $\alpha = 1$, then $E_1(t) = e^t$. When the argument $t \leq 0$, the ML function decreases monotonically, and for large values of t, we have

$$ E_{\alpha}(-t) \approx \frac{1}{\Gamma(1-\alpha)} \frac{1}{t}, \quad \alpha \neq 1,\ 0 < \alpha < 2 \tag{4} $$

The Laplace transform (5) allows an extension of transform pairs from the exponential function and integer powers of s toward the ML function and fractional powers of s[18]

$$ \mathcal{L}\{E_{\alpha}(\pm a t^{\alpha}\} = \frac{s^{\alpha-1}}{s^{\alpha} \mp a} \tag{5} $$

Based on these concepts of time-domain and frequency-domain tools, such as root locus,[25,26] Bode and Nyquist diagrams, as well as the concepts of stability and state-space, have been applied to fractional-order control systems for analysis and control synthesis.[24,27]

Equation (1) can be easily approximated numerically by[28,29]

$$ \begin{aligned} {}_a^{GL}D_t^{\alpha} f(t) &\approx {}_{(t-L)}^{GL}D_t^{\alpha} f(t) \\ &= T^{-\alpha} \sum_{m=0}^{N(t)} (-1)^m \binom{\alpha}{m} f(t - mT) \\ &= T^{-\alpha} \sum_{m=0}^{N(t)} c_m^{(\alpha)} f(t - mT) \end{aligned} \tag{6} $$

where T is the sampling period, L is the "memory length," and $N(t) = \min\{[t/h], [L/h]\}$.

The binomial coefficients $c_m^{(\alpha)}$ are given by[28]

$$ c_m^{(\alpha)} = \left(1 - \frac{1+\alpha}{m}\right) c_{m-1}^{(\alpha)}, \quad c_0^{(\alpha)} = 1 \tag{7} $$

Parameter L should be chosen using the criterion

$$ L \geq \frac{1}{\delta_0^2 \Gamma(\alpha)} \tag{8} $$

where δ_0 is the maximum admissible normalized error, given by

$$ \delta_0 = \frac{\left| {}_a^{GL}D_t^{\alpha} f(t) - {}_{(t-L)}^{GL}D_t^{\alpha} f(t) \right|}{M}, \quad M = \max_{[0,\infty]} |f(t)| \tag{9} $$

Fourier transform

The FT is a powerful and robust signal processing tool for the analysis of systems dynamics. The FT converts a time-domain signal or function, $f(t)$, to its frequency-domain counterpart, $F(j\omega)$[30–32]

$$ \mathcal{F}\{f(t)\} = F(j\omega) = \int_{-\infty}^{+\infty} f(t) e^{-j\omega t} dt \tag{10} $$

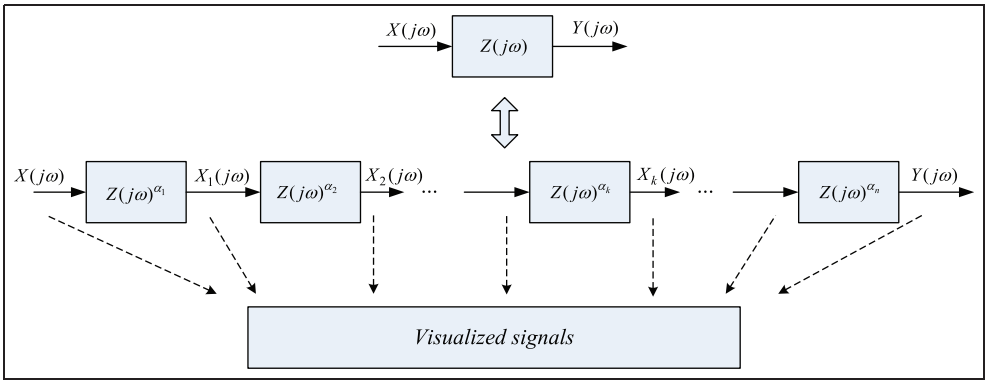

Figure 1. Fractionalization of a linear elemental block.

where $\mathcal{F}\{\cdot\}$ represents the Fourier operator and ω represents the angular frequency.

The inverse FT is given by

$$\mathcal{F}^{-1}\{F(j\omega)\} = f(t) = \frac{1}{2\pi}\int_{-\infty}^{+\infty} F(j\omega)e^{-j\omega t}d\omega \tag{11}$$

Applying the "differintegral" operator to both sides of equation (11), we obtain, within certain conditions[33,34]

$${}_0^{GL}D_t^{\alpha} f(t) = \mathcal{F}^{-1}\{(j\omega)^{\alpha}F(j\omega)\} \tag{12}$$

where $(j\omega)^{\alpha} = |\omega|^{\alpha}\exp[(sign(\omega)(j\alpha\pi/2)]$.

The FT has the advantage of being robust, allowing a direct interpretation of the processed data and being usable in a wide range of signals.

Fractionalization of elemental blocks

A control system is often represented graphically as a block diagram describing the system dynamic model. The block diagram includes no information about the physical construction of the system and is not unique. The main source of energy, as well as the energy flow, is not explicitly shown. Nevertheless, an individual block establishes a unilateral relationship between an input and an output signal, being assumed that there is no interaction between blocks.

Figure 1 represents the fractionalization of a linear elemental block, where $\alpha_i \in \mathbb{R}$, $i = 1, ..., n$, and $\sum_i^n \alpha_i = 1$.

The intermediate signal $X_k(j\omega)$ is given by

$$X_k(j\omega) = \left[\prod_{i=1}^{k} Z(j\omega)^{\alpha_i}\right] X(j\omega) \tag{13}$$

In the time domain, we have

$$x_k(t) = \mathcal{F}^{-1}\{X_k(j\omega)\} \tag{14}$$

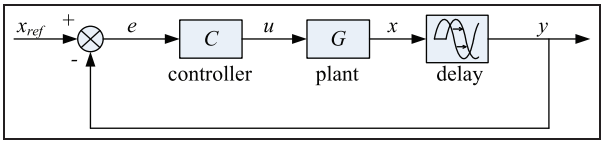

Figure 2. Linear control system with transport delay.

In the particular case of an integrator/differentiator elemental block, $x_k(t)$ can be computed directly in the time domain as

$$x_k(t) = {}_aD_t^{\alpha_1 + \alpha_2 + \cdots + \alpha_k} x(t) \tag{15}$$

Numerical simulation and computer visualization

For demonstrating the proposed concepts, we analyze in the sequel the behavior of two representative control systems. In sub-section "Fractionalization of a linear system," we consider a first-order linear plant with transport delay. In sub-section "Fractionalization of a nonlinear system," we address a nonlinear system comprising an inertia, Coulomb friction, transport delay, and backlash. The closed-loop time and frequency responses to a unit-step input are analyzed.

Fractionalization of a linear system

We start with the control system of Figure 2, where the plant, $G(s)$, and controller, $C(s)$, are given by[35]

$$G(s) = \frac{1}{1 + 20s}e^{-0.2s} \tag{16}$$

$$C(s) = 0.0880 + \frac{6.5185}{s^{0.6751} + 2.5881s^{0.6957}} \tag{17}$$

The controller is a fractional-order proportional–integral–derivative (PID), tuned by means of

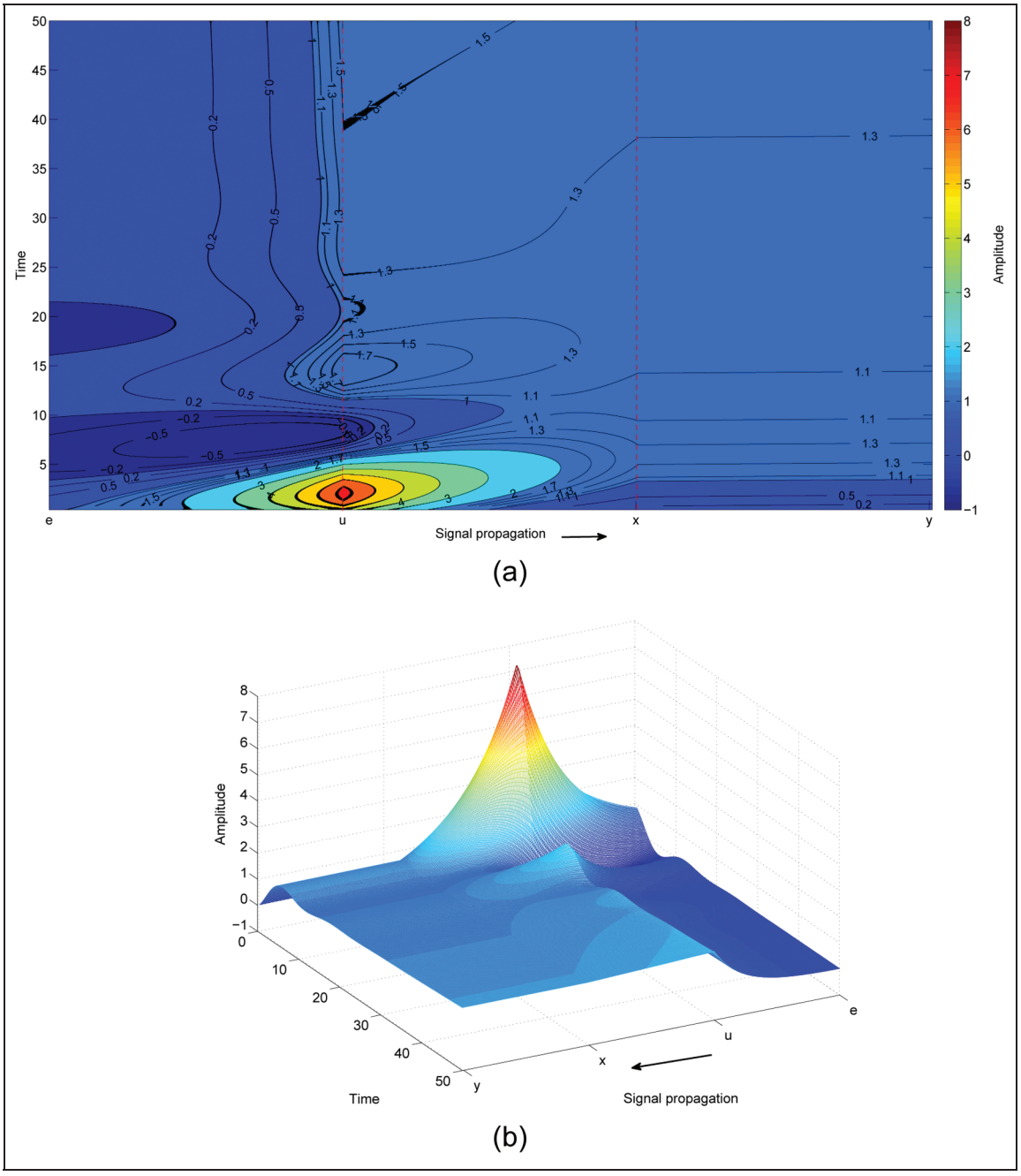

Figure 3. Time-domain representation of the signal propagating along the forward path of the linear control system in response to a unit-step input: (a) contour map and (b) 3D surface plot.

Ziegler–Nichols-type rules.[35] All units are expressed in the International System.

The three elemental blocks are fractionalized as described in sub-section "Fractionalization of elemental blocks," with α_i, $i = 1, ..., 101$, corresponding to numerical discretizations evenly spaced in the interval $[0, 1]$.

Figures 3 and 4 depict the new representation through the path $e \rightarrow u \rightarrow x \rightarrow y$. Figure 3 represents the signal propagating along the system structure in the time domain, that is, from the actuating error, e, toward the system output, y. To improve the readability, the results are depicted by means of both a contour map and a three-dimensional (3D) surface plot. In Figure 4, the signal evolution is expressed in the frequency domain. We identify the three stages of the traveling path: error $\rightarrow$ control action ($e \rightarrow u$) control action $\rightarrow$ plant output ($u \rightarrow x$), and plant output $\rightarrow$ system output ($x \rightarrow y$). The graphs show the signal moving along the system structure as a time/frequency-space wave. It should be noted that the method

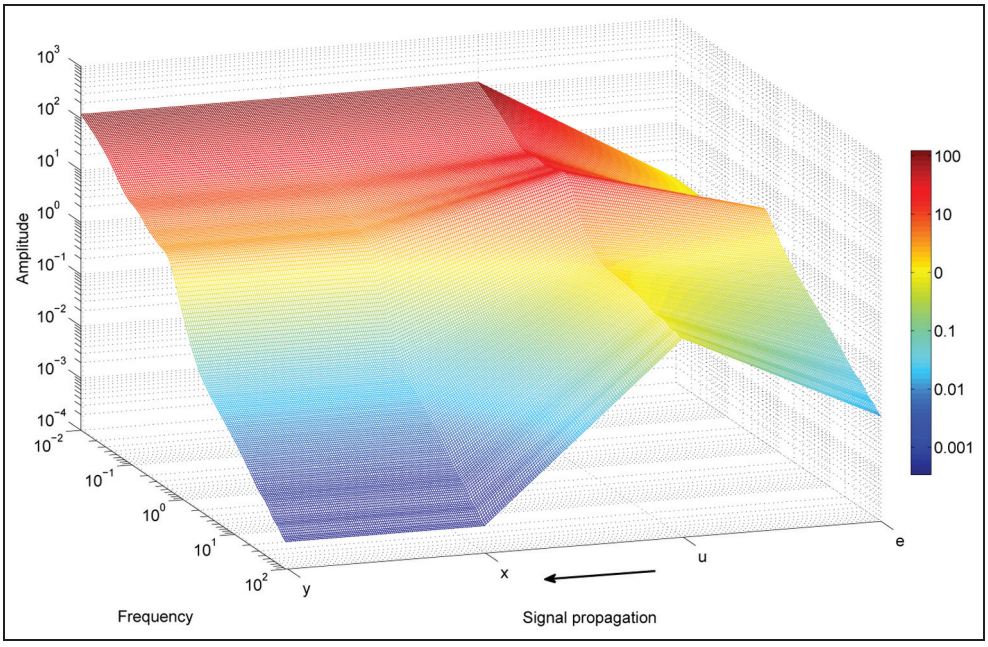

Figure 4. Frequency-domain representation of the signal propagating along the forward path of the linear control system in response to a unit-step input by means of a 3D surface plot.

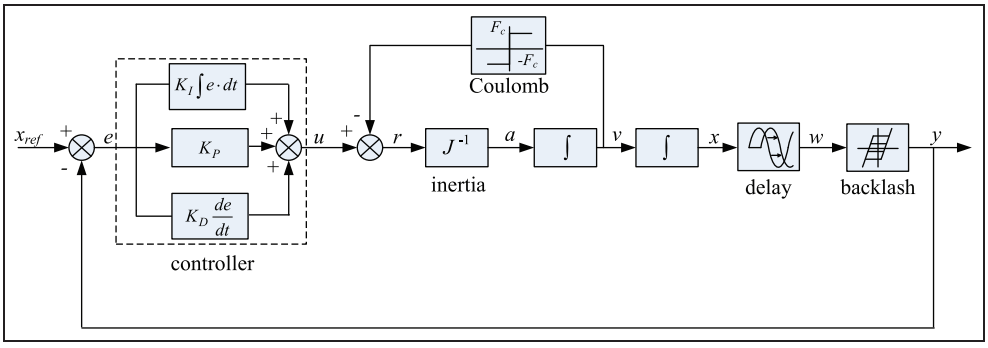

Figure 5. Block diagram of a feedback control system involving delay and nonlinearities.

generalizes and complements the classical visualization tools. The physical meaning, if any, of the signal away from the standard points $\{e, u, x, y\}$ is not considered here. Also, despite some graphical similarities with wavelet portraits, we should note that we are considering a technique formally distinct.

Fractionalization of a nonlinear system

We analyze now the nonlinear control system of Figure 5. This system comprises an integer-order PID controller, a double integrator, and a transport delay, τ. The nonlinearities include Coulomb friction force, F_C, and backlash, δ. Coulomb forces often cause undesirable vibration, as well as faulty operation. Backlash compromises system performance, originating delays, oscillations, and inaccuracies. Despite their importance, both phenomena are not yet fully understood, mainly due to the considerable randomness and the large variety of dynamic effects.[9,10,36,37]

The controller was tuned to yield an oscillatory stable response, thus sacrificing performance just to have a richer signal content for visualization. The system parameters are summarized in Table 1. All units are given in the International System.

As mentioned previously, the linear elemental blocks are fractionalized with α_i, $i = 1, ..., 101$, corresponding to numerical discretizations evenly spaced in the interval $[0, 1]$. The nonlinear blocks are not discretized.

Figures 6 and 7 show the signal propagation along the forward path of the block diagram, from the actuating error, e, toward the system output, y, in response to

Table 1. Parameters of the nonlinear control system.

PID			Inertia	Coulomb	Delay	Backlash
K_P	K_I	K_D	J	F_C	τ	δ
80	5	0.9	0.01	1	5×10^{-3}	5×10^{-2}

PID: proportional–integral–derivative.

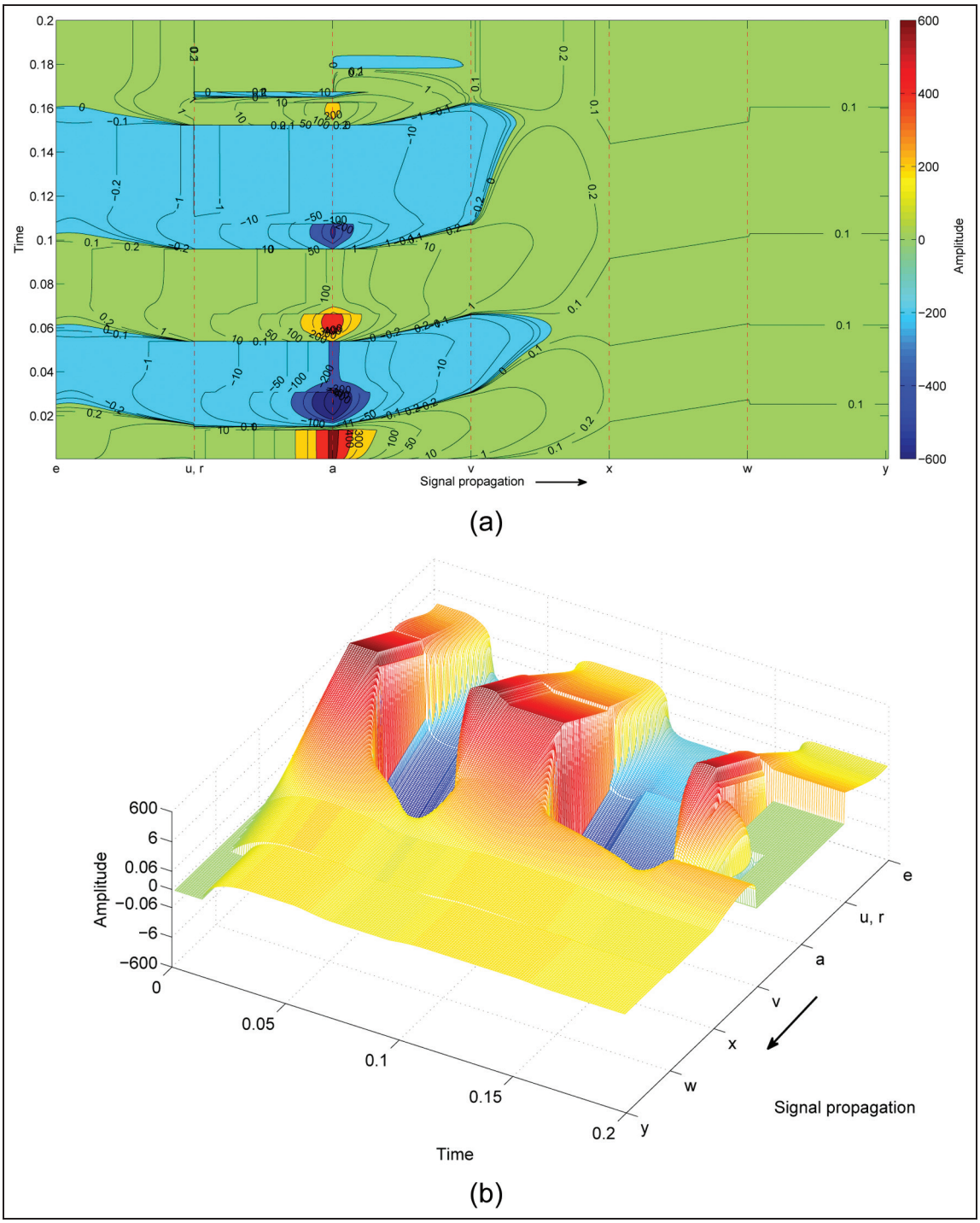

Figure 6. Time-domain representation of the signal propagating along the forward path of the nonlinear control system in response to a unit-step input: (a) contour map and (b) 3D surface plot with the z-axis scale implemented by means of the μ-law.

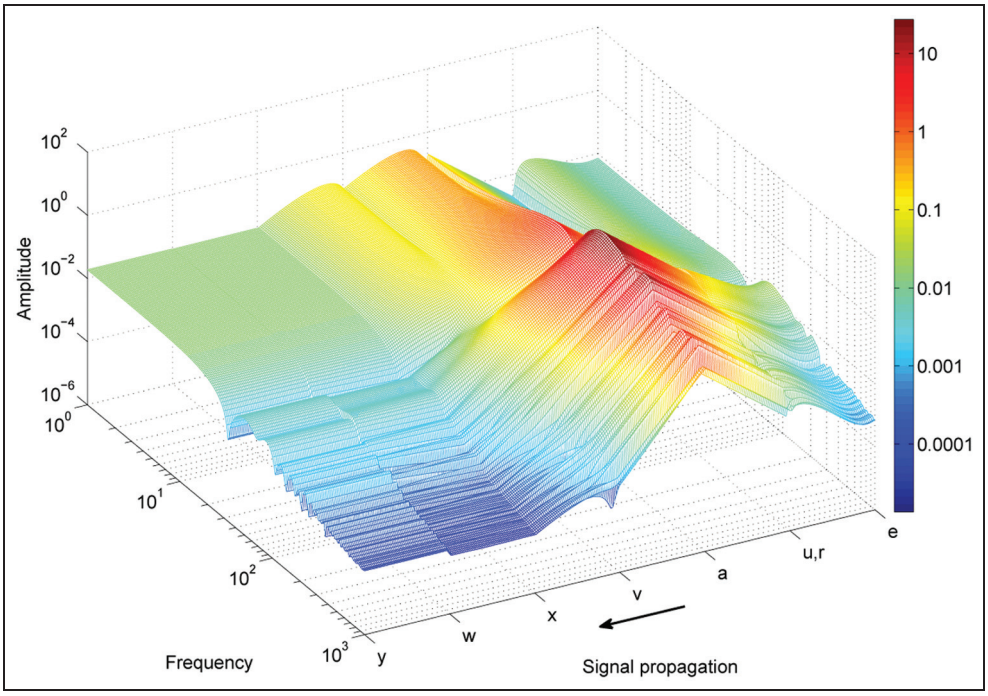

Figure 7. Frequency-domain representation of the signal propagating along the forward path of the nonlinear control system in response to a unit-step input by means of a 3D surface plot.

a unit-step reference, in time and frequency domains, respectively. To improve the readability, in Figure 6(a) we depict the results on a contour map, while in Figure 6(b) we represent the corresponding 3D mesh. Due to the broad range of amplitudes and the presence of negative values, we adopt a 3D chart with the z-axis scale implemented by means of the μ-law[38]

$$F(x) = sign(x)\frac{\log(1+\mu|x|)}{\log(1+\mu)} \tag{18}$$

where $\mu = 255$.

We identify six stages on the signal traveling path. In the portion, error $\rightarrow$ control action ($e \rightarrow u$) we observe the controller behavior. First, the integral contribution is more effective, corresponding to contour lines with positive slope in Figure 6(a), and then the derivative action dominates, inverting the slope of the lines. At the points $\{u, r\}$ (corresponding to the left and right sides of the sum block), a discontinuity occurs caused by the Coulomb force, F_C. In the path connecting both sides of the block J^{-1} ($r \rightarrow a$), we visualize the effect of the inertia. The amplitude of the signal increases, reaching its maximum value that corresponds to the acceleration, a. In the next two portions, that is, in the path acceleration $\rightarrow$ input of delay block ($a \rightarrow x$), the signal is fractionally integrated, and decreases in amplitude. In the branch ($x - w$), the signal travels through the delay block, and we observe that the slope of the contour lines is proportional to the delay, δ. Finally, at point w, a discontinuity occurs caused by the backlash, τ, and the contour lines become horizontal, meaning that we can visualize the signal just before and after the backlash block, but we are not able to observe the traveling signal across the block.

Conclusion

This article formulated a novel visualization technique inspired in the FC paradigm that is particularly useful in the presence of nonlinear dynamics. The proposed methodology determines the signal propagating as a time/frequency-space wave within the structure of a controlled system. Linear and nonlinear closed-loop control systems were analyzed based on the time and frequency responses under the action of a reference step input signal. The method is an abstract scheme, and the results are to be interpreted as a new visualization concept that extends the capabilities of the classical tools. Therefore, obtaining a physical meaning is not the goal of this study but to open a new research procedure to the classical integer modus operandi. Further research may address more complex control systems, involving distinct nonlinearities, or the embedding of the proposed fractionalization scheme with different signal analysis tools or computer visualization techniques.

Declaration of conflicting interests

The author(s) declared no potential conflicts of interest with respect to the research, authorship, and/or publication of this article.

Funding

The author(s) received no financial support for the research, authorship, and/or publication of this article.

References

1. Dorf RC and Bishop RH. *Modern control systems*. Reading, MA: Pearson (Addison-Wesley), 1998.
2. Ogata K. *Discrete-time control systems*, vol. 2. Englewood Cliffs, NJ: Prentice Hall, 1995.
3. Franklin GF, Powell JD and Workman ML. *Digital control of dynamic systems*, vol. 3. Menlo Park, CA: Addison-Wesley, 1998.
4. Skogestad S and Postlethwaite I. *Multivariable feedback control: analysis and design*, vol. 2. New York: Wiley, 2007.
5. Nijmeijer H and Van der Schaft A. *Nonlinear dynamical control systems*. New York, NY: Springer Science + Business Media, 2013.
6. Slotine JJE and Li W. *Applied nonlinear control*, vol. 199. Englewood Cliffs, NJ: Prentice Hall, 1991.
7. Khalil HK and Grizzle J. *Nonlinear systems*, vol. 3. Englewood Cliffs, NJ: Prentice Hall, 1996.
8. Freeman RA and Kokotovic PV. *Robust nonlinear control design: state-space and Lyapunov techniques*. Basel: Springer Science + Business Media, 2008.
9. Duarte FB and Machado JT. Fractional describing function of systems with Coulomb friction. *Nonlinear Dynam* 2009; 56: 381–387.
10. Duarte FB and Machado JT. Describing function of two masses with backlash. *Nonlinear Dynam* 2009; 56: 409–413.
11. Machado JT. Fractional order describing functions. *Signal Process* 2015; 107: 389–394.
12. Baleanu D, Diethelm K, Scalas E, et al. *Models and numerical methods*, vol. 3. Singapore: World Scientific, 2012.
13. Kenneth M and Ross B. *An introduction to the fractional calculus and fractional differential equations*. New York: Wiley, 1993.
14. Mainardi F. *Fractional calculus and waves in linear viscoelasticity: an introduction to mathematical models*. Singapore: World Scientific, 2010.
15. Luo Y and Chen Y. *Fractional order motion controls*. Chichester: John Wiley Sons, 2012.
16. Sheng H, Chen Y and Qiu T. *Fractional processes and fractional-order signal processing: techniques and applications*. London: Springer Science + Business Media, 2011.
17. Ionescu CM. *The human respiratory system: an analysis of the interplay between anatomy, structure, breathing and fractal dynamics*. London: Springer Science + Business Media, 2013.
18. Lopes AM and Machado JT. Fractional order models of leaves. *J Vib Contr* 2014; 20: 998–1008.
19. Silva MF, Machado JT and Lopes A. Fractional order control of a hexapod robot. *Nonlinear Dynam* 2004; 38: 417–433.
20. Lopes AM, Machado JT, Pinto CM, et al. Fractional dynamics and MDS visualization of earthquake phenomena. *Comput Math Appl* 2013; 66: 647–658.
21. De Oliveira EC and Machado J. A review of definitions for fractional derivatives and integrals. *Math Probl Eng* 2014; 2014: 238459.
22. Machado JT, Kiryakova V and Mainardi F. Recent history of fractional calculus. *Comm Nonlinear Sci Numer Simulat* 2011; 16: 1140–1153.
23. Valério D, Trujillo JJ, Rivero M, et al. Fractional calculus: a survey of useful formulas. *Eur Phys J Spec Top* 2013; 222: 1827–1846.
24. Petras I. *Fractional-order nonlinear systems: modeling, analysis and simulation*. Berlin: Springer Science + Business Media, 2011.
25. Merrikh-Bayat F and Afshar M. Extending the root-locus method to fractional-order systems. *J Appl Math* 2008; 2008: 528934.
26. Lopes AM and Tenreiro Machado J. Root locus practical sketching rules for fractional-order systems. *Abstr Appl Anal* 2013; 2013: 102068.
27. Raynaud HF and Zerganoh A. State-space representation for fractional order controllers. *Automatica* 2000; 36: 1017–1021.
28. Dorcak L. Numerical models for the simulation of the fractional-order control systems. arXiv:math/0204108 (math.OC), 2002.
29. Podlubny I. *Fractional differential equations*. San Diego, CA: Academic Press, 1999.
30. Schafer RW and Oppenheim AV. *Discrete time signal processing*. Englewood Cliffs, NJ: Prentice Hall, 1989.
31. Chen CT. *Digital signal processing: spectral computation and filter design*. New York: Oxford University Press, 2000.
32. Van Loan C. *Computational frameworks for the fast Fourier transform*, vol. 10. Philadelphia, PA: SIAM, 1992.
33. Tseng CC, Pei SC and Hsia SC. Computation of fractional derivatives using Fourier transform and digital FIR differentiator. *Signal Process* 2000; 80: 151–159.
34. Ortigueira MD and Trujillo JJ. Generalized GL fractional derivative and its Laplace and Fourier transform. In: *ASME 2009 international design engineering technical conferences and computers and information in engineering conference*, San Diego, USA, 30 August 2009, pp.1227–1231. New York: ASME.
35. Valério D and Da Costa JS. Tuning of fractional PID controllers with Ziegler–Nichols-type rules. *Signal Processing* 2006; 86: 2771–2784.
36. Armstrong-Hélouvry B, Dupont P and De Wit CC. A survey of models, analysis tools and compensation methods for the control of machines with friction. *Automatica* 1994; 30: 1083–1138.
37. Leine R, Van de and Wouw N. Stability properties of equilibrium sets of non-linear mechanical systems with dry friction and impact. *Nonlinear Dynam* 2008; 51: 551–583.
38. Deepa T and Kumar R. Performance analysis of μ-law companding & SQRT techniques for M-QAM OFDM systems. In: *2013 international conference on emerging trends in computing, communication and nanotechnology (ICE-CCN)*, Tirunelveli, India, 25–26 March 2013, pp.303–307. New York: IEEE.